Fractional-order photonic differentiator using an on-chip microring resonator

Aoling Zheng,[1] Jianji Dong,[1,*] Linjie Zhou,[2] Xi Xiao,[3] Qi Yang,[3] Xinliang Zhang,[1] and Jianping Chen[2]

[1]*Wuhan National Laboratory for Optoelectronics, Huazhong University of Science and Technology, Wuhan 430074, China*

[2]*State Key Laboratory of Advanced Optical Communication Systems and Networks, Department of Electronic Engineering, Shanghai Jiao Tong University, Shanghai 200240, China*

[3]*State Key Laboratory of Optical Communication Technologies and Networks, Wuhan Research Institute of Posts & Telecommunications, Wuhan 430074, China*

**Corresponding author: jjdong@mail.hust.edu.cn*

Received August 12, 2014; revised September 29, 2014; accepted October 14, 2014; posted October 14, 2014 (Doc. ID 220882); published October 31, 2014

A tunable temporal photonic fractional differentiator using a silicon-on-isolator (SOI) electrically tuned microring resonator (MRR) is proposed and experimentally demonstrated. Through changing the voltage applied on the MRR, the fractional order of the photonic differentiator can be continuously tuned. The proposed fractional-order differentiator is demonstrated experimentally with Gaussian pulse injection and rectangular pulse injection, respectively. The small deviation shows the feasibility of our photonic differentiator with an integrated silicon MRR. © 2014 Optical Society of America

OCIS codes: (200.4740) Optical processing; (230.1150) All-optical devices; (320.5540) Pulse shaping.
http://dx.doi.org/10.1364/OL.39.006355

With the rapid development of data centers and high-performance computers, silicon photonics has grown as an ideal solution for high-bandwidth on-chip interconnects and energy-efficient telecommunications. On-chip short-reach communication and computing with silicon waveguides become very important, where very basic optical processors, such as optical differentiators, integrators, and logic units, are highly desirable. A temporal photonic differentiator (DIFF) is a basic operator that performs real-time DIFF of the field envelope of an optical signal. Photonic DIFF is attracting lots of interest due to its wide applications in numerous fields such as pulse characterization, ultrafast signal generation, and ultrahigh-speed coding [1–3].

Photonic DIFF can be categorized with integer-order DIFF and fractional-order DIFF. Integer-order DIFF has been well known and widely proposed, including with the use of a long-period fiber grating [4], a phase-shifted fiber Bragg grating [5], an interferometer [6], a semiconductor optical amplifier [7], a silicon microring resonator (MRR) [8,9], and a directional coupler [10]. Fractional-order DIFF is the extension of integer-order DIFF, which can accomplish what integer-order differentiation cannot do [11]. Originating from mathematics, fractional-order DIFF can be used in fractal geometry, chaos circuits, and edge detection of image, and so on [12–14]. Thus, fractional-order DIFF is also significant in temporal optical signal processing. Currently, the fractional-order DIFF has been implemented with different methods such as asymmetrical phase-shifted fiber Bragg grating [15], tilted fiber Bragg grating [16], silicon-on-isolator (SOI) MRR with a multimode interferometer (MMI) coupler [17], and electrically tuned Mach–Zenhder interferometer (MZI) [18]. Among these schemes, silicon-based waveguide is preferred to fulfill the chip-level optical processor, which can offer intrinsic advantages of compact footprint, good integration capability, and compatibility with complementary metal-oxide semiconductor (CMOS) technology. For the first time to our knowledge, [17] presented a ring-resonator-based fractional-order DIFF with a continuously tunable order. The tuning range of fractional order can cover 0.37–1.3 by changing the polarization state of input light, but this scheme is not suitable for circular polarized lights or a polarization convertor is needed before the MRR. Zheng *et al.* [18] demonstrated a tunable fractional-order DIFF based on an electrically tuned MZI. The DIFF has an operation bandwidth of several hundred GHz but with very low energy efficiency of processing signals with narrow bandwidth.

In this Letter, we present a tunable fractional-order DIFF based on an electrically tuned SOI MRR. When different voltages are applied on the MRR, the carrier in the ring waveguide is changed to vary the internal refractive index and loss, which leads to the change of Q-factor and phase shift at resonant frequencies. Thus, a fractional-order DIFF can be implemented. Note that the order tunability is obtained by changing the voltage applied on the MRR, and it is not related to the polarization state of lights. Additionally, the MRR has a rather high Q-factor with a narrow operational bandwidth. However, it has good energy efficiency because of its high spectral slope.

A temporal DIFF is a filtering device that provides the derivative of the input pulse. An Nth-order optical temporal DIFF is a filter with a spectral transfer function of

$$H(\omega) = [j(\omega - \omega_0)]^N, \tag{1}$$

where N is not necessarily an integer generalized to fractional-order differentiation, ω is the optical angular frequency, ω_0 is the carrier angular frequency, and $j = \sqrt{-1}$. This transfer function indicates an exact $N\pi$ phase shift in the phase response at the central angular frequency ω_0. We demonstrate here that an optical filter with a frequency response given by (1) can be implemented using an SOI MRR.

Mathematically, the frequency response of an MRR can be expressed as [19]

$$T = \frac{E_{\text{out}}}{E_{\text{in}}} = \frac{r - \alpha e^{j\varphi}}{1 - \alpha r e^{j\varphi}}, \tag{2}$$

where $\varphi = 2\pi n_{\text{eff}} L/\lambda$ is the total roundtrip phase accumulation, L is the ring-cavity length, α is the ring-propagation loss factor, n_{eff} is the wavelength effective index, λ is the wavelength in vacuum, and r is the transmission coefficient.

When $\alpha < r$, MRR works in the under-coupling regime, and a phase shift of less than π can be achieved. When $\alpha > r$, a phase shift of more than π can be achieved since the MRR works in the over-coupling regime. When we apply voltage on the doped-silicon MRR and increase the voltage, the loss of the ring waveguide increases and thus the ring-propagation loss factor α decreases. The amplitude and phase responses of the MRR are shown in Figs. 1(a) and 1(b), where the propagation-loss factor varies. The transmission coefficient is constant. As can be seen in Fig. 1(b), by decreasing α from 0.968 to 0.952, the phase shift is changed from 1.5π to about 0.6π, thus a fractional-order DIFF with an order tunable from 1.5 to 0.6 can be implemented. It should be noted that for the implementation of a DIFF, the phase response is more important than the magnitude response [20,21].

The magnitude and phase spectra of an MRR with $\alpha = 0.959$ and $r = 0.960$ corresponding to DIFF with a fractional order of 0.90 are shown in Figs. 2(a) and 2(b). The magnitude and phase responses of the MRR fit well with that of the ideal fractional-order DIFF ($N = 0.9$) within a certain bandwidth, indicating the proposed DIFF has a device-operation bandwidth (DOB) [22]. Figure 2(c) shows the output differentiated waveform when the input Gaussian pulse has a full width at half-maximum (FWHM) of 30 ps, which accords well with the ideal fractional-order differentiation with an order of 0.90. The deviation of the proposed DIFF output from the ideal DIFF as a function of input FWHM is shown in Fig. 2(d). It can be seen that the deviation decreases when the FWHM of the input pulse increases. This is because

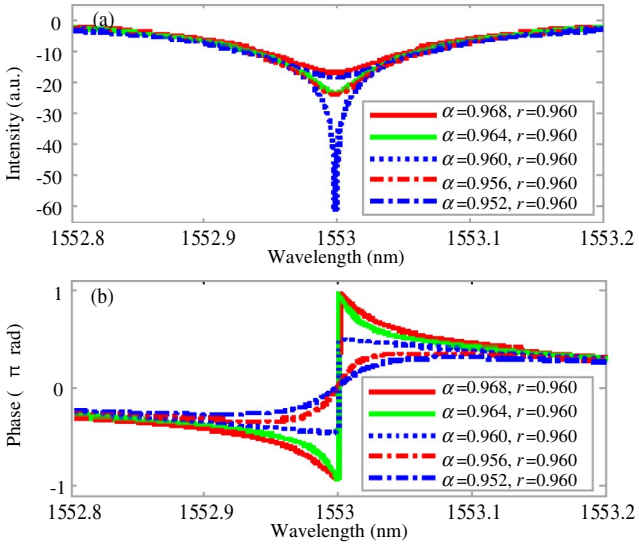

Fig. 1. Magnitude (a) and phase response (b) of the MRR operating at 1553 nm for different values of α.

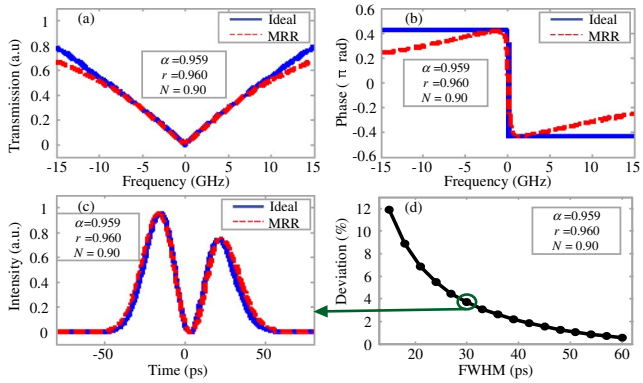

Fig. 2. (a) Magnitude response and (b) phase response of the transmission spectrum of the MRR, with $\alpha = 0.959$ and $r = 0.960$. The solid line shows the magnitude and phase response of an ideal DIFF. (c) Simulated output pulse from the MRR of an input Gaussian pulse with a FWHM of 30 ps. The solid line shows the output pulse from an ideal DIFF. The fractional order is 0.90. (d) Deviations of the simulated output pulse from the ideal output pulse for input pulse with different FWHM.

the input pulse with smaller FWHM has the larger bandwidth, which may be larger than the DOB of the DIFF.

We then employ an on-chip MRR structure to implement fractional-order differentiation. We design and fabricate the MRR on an SOI wafer. The thickness of the top silicon and the buried oxide layer of the SOI wafer are 220 nm and 2 μm, respectively. We employ deep ultraviolet (DUV) photolithography using a 248-nm stepper to define the waveguide patterns, and then anisotropic dry etch of silicon is employed. Boron and phosphorus ion implantations are performed to form the highly p-type and n-type doped regions. Also the slab layer is etched outside the p–i–n junctions to confine the current flow around the ring waveguide. Finally, contact holes are etched and aluminum is deposited to form the metal connection. The whole fabrication process is done using CMOS-compatible processes. We use a vertical grating-coupling method to couple the fiber and the silicon MRR. Figure 3 shows the micrographs of (a) the fabricated MRR and (b) the zoom-in ring region. The scaling bars are shown.

The measured magnitude response of the MRR is shown in Fig. 4. We apply voltages of 0.00, 0.85, 0.90, and 0.95 V on the MRR, respectively. Comparing the amplitude responses in Figs. 1(a) and 4, we can see that when the applied voltage is 0 V, there is the deepest frequency notch, indicating a phase shift closest approach to π at the frequency notch. As the applied voltage

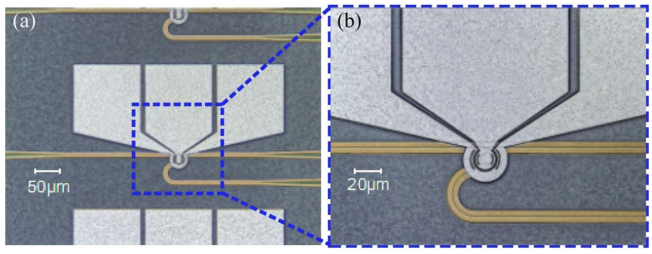

Fig. 3. (a) Microscope image of the fabricated MRI and (b) microscope image of the zoom-in ring region.

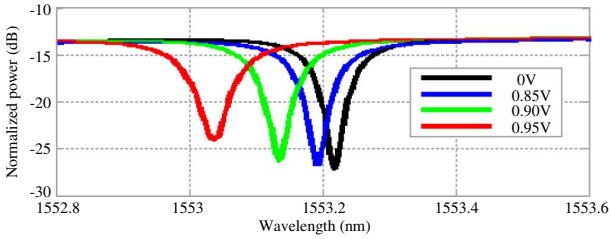

Fig. 4. Measured magnitude response of the MRR in transmission at different voltages.

increases, the notch depth of the MRR decreases. When the voltage is changed by 0.1 V, the resonant wavelength is shifted by about 0.08 nm correspondingly. Therefore, the optical carrier of the signal to be differentiated should be tuned correspondingly. The total loss (including the coupling losses on both sides) of the MRR chip is about 14 dB. The 3-dB bandwidth is about 10 GHz. Due to the hardware restraint, the phase response of the MRR chip was not measured. However, we can deduce from Figs. 1 and 4 that the MRR has a varied phase shift at the resonant frequency by applying different voltages.

The experiment setup for the fractional-order DIFF is shown in Fig. 5. A continuous wave (CW) beam generated by the tunable laser source (TLS) with a precisely tuning resolution of 100 MHz is externally modulated by two cascaded MZMs driven with self-coded data signal from a bit-pattern generator (BPG). The frequency of the CW beam is aligned to the resonant frequency of the MRR according to the device-operation principle. An erbium-doped fiber amplifier (EDFA) connected at the output of the MZMs is used to amplify the optical signal. Subsequently, the generated optical signal is coupled into the MRR using the vertical grating-coupling method [23]. Polarization controllers (PCs) connected to the TLS and EDFA are to control and tune the polarization state of the input light to the MZMs and to the MRR, respectively. Additionally, a direct-current voltage source is used to provide different voltages applied on the MRR. Then the output signal at the through port of the MRR is amplified by an EDFA and finally analyzed by a digital communications analyzer (Agilent DCA86100C).

First, the BPG drives the two MZMs to generate a Gaussian pulse train with a FWHM of 30 ps and a repetition frequency of 10 GHz, as shown in Fig. 6(a). When we apply voltages of 0.00, 0.85, 0.90, and 0.95 V on the MRR, we measure the temporal waveforms of DIFFs with fractional orders of 0.97, 0.80, 0.63, and 0.58, respectively, which are shown in Figs. 6(b)–6(e), respectively. It can be seen that the measured differentiated pulses fit well with the simulated pulses. Since the resonant wavelength is shifted when we apply different voltage on the

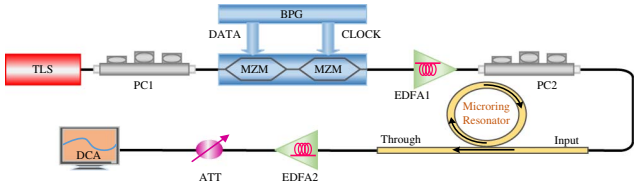

Fig. 5. Experimental setup for the fractional-order DIFF with on-chip MRR structure.

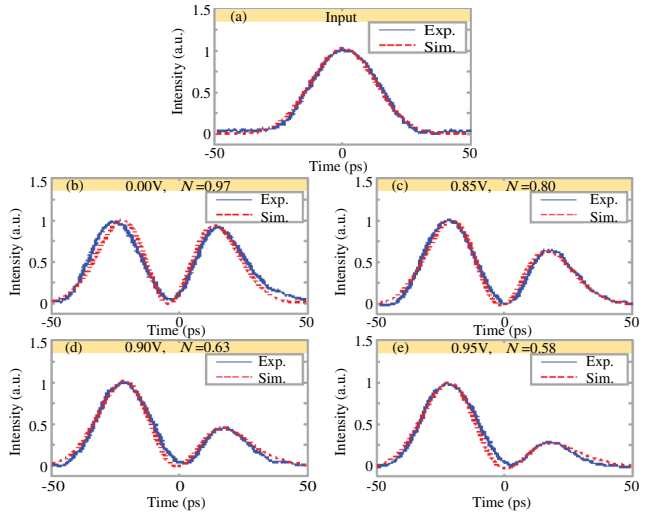

Fig. 6. (a) Input Gaussian pulse with an FWHM of 30 ps, and the differentiated pulses at the different voltages corresponding to differentiation orders of (b) $N = 0.97$, (c) $N = 0.80$, (d) $N = 0.63$, and (e) $N = 0.58$.

MRR, we first observe the MRR spectral notch and fix it, and then tune the TLS wavelength at the same wavelength. For example, Fig. 7 shows the spectra of the input Gaussian pulse and the output pulse with a DIFF order of 0.97. The notch wavelength and the TLS wavelength are both at 1553.22 nm. One can see the input signal carrier is well aligned with the MRR resonant notch, and the carrier is deeply suppressed at the output spectrum. It should be noted that when no voltage is applied on the MRR, the DIFF order is 0.97 but not 1, which depends on the relationship between the transmission coefficient r and the ring-propagation loss factor α. One can design the gap between the straight waveguide and the ring waveguide of the MRR so that $\alpha = r$. Then, we can obtain a DIFF with $N = 1$. Theoretically, the phase jump at resonant wavelength can be tuned freely by applying different voltages. However, in amplitude response of the MRR, the notch depth becomes small if α and r are mismatched much. In this case, the optical carrier could not be suppressed and the DIFF function then fails. Thus, the fractional-order tunability actually has a finite range.

Then, the BPG drives the two MZMs to generate a rectangular pulse train with a pulsewidth of 70 ps and a repetition frequency of 5 GHz, as shown in Fig. 8(a). When we apply voltages with 0.0, 0.85, and 0.90 V on the MRR, and fine-tune the TLS wavelength to align with the resonant notch, the output differentiated waveforms are as shown in Figs. 8(b)–8(d). The simulated

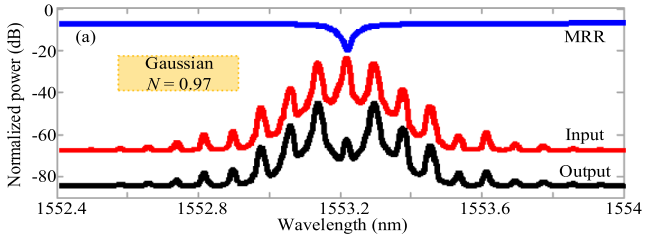

Fig. 7. Measured spectra of the MRR, the input Gaussian pulse, and the output pulse.

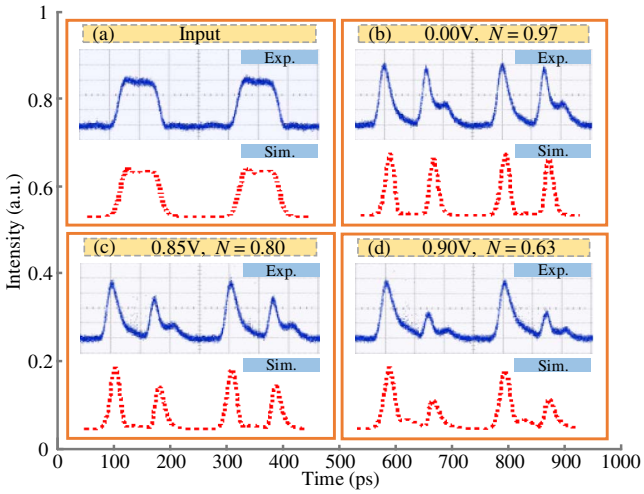

Fig. 8. (a) Input rectangular pulse with an FWHM of 70 ps, and the differentiated pulses at the different voltages corresponding to differentiation orders of (b) $N = 0.97$, (c) $N = 0.80$, and (d) $N = 0.63$.

waveforms of fractional-order differentiation are also shown, whose fractional orders are $N = 0.97$, 0.80, and 0.63, respectively. One can see that there is a good agreement between the measured pulses and the ideal DIFFs, except for a small discrepancy in the pulse tails.

From Fig. 4, the 3 dB bandwidth of the MRR is about 10 GHz. As the phase response is more important than the magnitude response for the implementation of a DIFF, the proposed DIFF is expected to differentiate an input pulse with a bandwidth of tens of GHz. One can see from Fig. 7 that the input Gaussian pulse has a bandwidth of about 30 GHz, but the DIFF deviation is very tiny. We also notice that a practical DIFF has not only a maximum-operation bandwidth, i.e., DOB, but also a bandwidth lower limitation from power efficiency, because the larger DOB normally has a lower spectral slope, resulting in a lower power efficiency for the differentiated signals [1,22]. Thus, there will be huge energy loss if a DIFF with a bandwidth of several hundred gigahertz or even terahertz is used to process a signal with a bandwidth of only tens of gigahertz. The output power might be quite weak or even cannot be detected. Our scheme has an operation bandwidth of tens of gigahertz and high power efficiency within this bandwidth range.

In summary, a silicon photonics-based continuously tunable fractional-order temporal DIFF was proposed and experimentally demonstrated. The key to achieving the differentiation-order tuning was based on the changing of the voltage applied on the ring, which led to the change of the ring-propagation-loss factor, resulting in the changing of the phase shift. The proposed DIFF is expected to have an operation bandwidth of tens of gigahertz and have high energetic efficiency. It was demonstrated that the fractional order of a Gaussian pulse with a pulse width of 30 ps and a rectangular pulse with a pulse width of 70 ps could be tuned from 0.58 to 0.97 and 0.63 to 0.97, respectively.

This work was partially supported by the National Natural Science Foundation of China (Grant No. 61475052, Grant No. 11174096), National Basic Research Program of China (Grant No. 2011CB301704), the Program for New Century Excellent Talents in Ministry of Education of China (Grant No. NCET-11-0168), and the Foundation for the Author of National Excellent Doctoral Dissertation of China (Grant No. 201139).

References

1. J. Azaña, IEEE Photon. J. **2**, 359 (2010).
2. R. Slavík, Y. Park, M. Kulishov, R. Morandotti, and J. Azaña, Opt. Express **14**, 10699 (2006).
3. N. Q. Ngo, S. F. Yu, S. C. Tjin, and C. H. Kam, Opt. Commun. **230**, 115 (2004).
4. J. Azaña and M. Kulishov, Electron. Lett. **41**, 1368 (2005).
5. N. K. Berger, B. Levit, B. Fischer, M. Kulishov, D. V. Plant, and J. Azaña, Opt. Express **15**, 371 (2007).
6. Y. Park, J. Azaña, and R. Slavík, Opt. Lett. **32**, 710 (2007).
7. J. Xu, X. Zhang, J. Dong, D. Liu, and D. Huang, Opt. Lett. **32**, 1872 (2007).
8. F. Liu, T. Wang, L. Qiang, T. Ye, Z. Zhang, M. Qiu, and Y. Su, Opt. Express **16**, 15880 (2008).
9. J. Dong, A. Zheng, D. Gao, S. Liao, L. Lei, D. Huang, and X. Zhang, Opt. Lett. **38**, 628 (2013).
10. T.-J. Ahn and J. Azaña, Opt. Express **19**, 7625 (2011).
11. C. Cuadrado-Laborde, Opt. Quantum Electron. **40**, 983 (2008).
12. M. Giona and H. E. Roman, J. Phys. A **25**, 2093 (1992).
13. M. S. Tavazoei, M. Haeri, S. Jafari, S. Bolouki, and M. Siami, IEEE Trans. Ind. Electron. **55**, 4094 (2008).
14. C. B. Gao, J. L. Zhou, J. R. Hu, and F. N. Lang, in *IET Image Processing* (Institution of Engineering and Technology, 2011), pp. 261–272.
15. C. Cuadrado-Laborde and M. V. Andrés, Opt. Lett. **34**, 833 (2009).
16. M. Li, L.-Y. Shao, J. Albert, and J. Yao, IEEE Photon. Technol. Lett. **23**, 251 (2011).
17. H. Shahoei, D.-X. Xu, J. H. Schmid, and J. Yao, IEEE Photon. Technol. Lett. **25**, 1408 (2013).
18. A. Zheng, T. Yang, X. Xiao, Q. Yang, X. Zhang, and J. Dong, Opt. Express **22**, 18232 (2014).
19. A. Yariv, Electron. Lett. **36**, 321 (2000).
20. A. V. Oppenheim and J. S. Lim, Proc. IEEE **69**, 529 (1981).
21. H. Shahoei, J. Albert, and J. Yao, IEEE Photon. Technol. Lett. **24**, 730 (2012).
22. R. Ashrafi and J. Azaña, Opt. Express **20**, 2626 (2012).
23. D. Taillaert, F. V. Laere, M. Ayre, W. Bogaerts, D. V. Thourhout, P. Bienstman, and R. Baets, Jpn. J. Appl. Phys. **45**, 6071 (2006).